Regulatory T cells suppress muscle inflammation and injury in muscular dystrophy.

MUSCULAR DYSTROPHY

Regulatory T cells suppress muscle inflammation and injury in muscular dystrophy

S. Armando Villalta,[1]* Wendy Rosenthal,[1] Leonel Martinez,[2] Amanjot Kaur,[1] Tim Sparwasser,[3] James G. Tidball,[4] Marta Margeta,[5] Melissa J. Spencer,[2] Jeffrey A. Bluestone[1,5,6]

We examined the hypothesis that regulatory T cells (T_{regs}) modulate muscle injury and inflammation in the mdx mouse model of Duchenne muscular dystrophy (DMD). Although T_{regs} were largely absent in the muscle of wild-type mice and normal human muscle, they were present in necrotic lesions, displayed an activated phenotype, and showed increased expression of interleukin-10 (IL-10) in dystrophic muscle from mdx mice. Depletion of T_{regs} exacerbated muscle injury and the severity of muscle inflammation, which was characterized by an enhanced interferon-γ (IFN-γ) response and activation of M1 macrophages. To test the therapeutic value of targeting T_{regs} in muscular dystrophy, we treated mdx mice with IL-2/anti–IL-2 complexes and found that T_{regs} and IL-10 concentrations were increased in muscle, resulting in reduced expression of cyclooxygenase-2 and decreased myofiber injury. These findings suggest that T_{regs} modulate the progression of muscular dystrophy by suppressing type 1 inflammation in muscle associated with muscle fiber injury, and highlight the potential of T_{reg}-modulating agents as therapeutics for DMD.

INTRODUCTION

Duchenne muscular dystrophy (DMD) is a lethal muscle degenerative disorder that is caused by loss-of-function mutations in the dystrophin gene (*1*, *2*). Hypomorphic dystrophin mutations result in a milder clinical phenotype known as Becker muscular dystrophy (BMD) (*3*). DMD is characterized by a progressive deterioration of muscle function and strength, loss of ambulation by the second decade of life, and death in the early to mid-20s. Despite a kinetic difference in the progressive deterioration of muscle mass/function and the development of fatty fibrotic deposits between mdx mice and DMD/BMD patients, mdx mice similarly lack dystrophin and develop a muscular dystrophy that shares many pathological features with the human disease (*4*). Studies using the mdx mouse model have revealed that the physical and cellular basis of muscle degeneration can be attributed to loss of sarcolemmal integrity, increased susceptibility to oxidative stress, and severe myofiber degeneration and inflammation (*5*–*7*).

Although the lack of dystrophin protein is the primary defect responsible for the development of muscular dystrophy, secondary disease processes such as muscle inflammation contribute greatly to the pathogenesis of DMD (*8*). The leukocyte infiltrate of dystrophic muscle is heterogeneous, comprising neutrophils, eosinophils, macrophages, and $CD8^+$ and $CD4^+$ T cells (*9*–*12*). Depletion of specific immune cell populations with anti-F4/80 or anti–Gr-1 (myeloid cell–specific) or with anti-CD4 or anti-CD8 (T cell–specific) antibodies has shown that reducing the numbers of myeloid cells or T cells in dystrophic muscle decreased the proportion of necrotic myofibers in mdx mice (*10*–*12*). Similarly, broad glucocorticosteroid-mediated immunosuppression in DMD patients and mdx mice delays the severity and progression of muscular dystrophy, likely involving suppression of muscle inflammation and direct effects on muscle function (*13*–*15*).

In addition to promoting muscle injury during muscular dystrophy, the immune system also facilitates muscle regeneration and repair (*16*). This dichotomous role of the immune system in muscle disease may be partly explained by the development of type 1 and type 2 inflammatory responses that promote muscle damage and repair, respectively. Type 1 inflammation is characterized by the increased expression of interferon-γ (IFN-γ) and is counterregulated by type 2 inflammatory cytokines such as interleukin-4 (IL-4) and IL-13 and the antiinflammatory cytokine IL-10. Although several studies have elucidated how these inflammatory responses mediate injury and repair (*17*–*21*), it is not clear how the balance between type 1 and type 2 inflammatory responses is regulated in muscle or what regulatory role lymphocytes exert on this balance.

Regulatory T cells (T_{regs}) are candidate immunosuppressive lymphocytes that have the functional capacity to modulate dystrophinopathy by regulating the balance between type 1 and type 2 inflammatory responses. They are a specialized subset of $CD4^+$ T cells whose lineage specification is dependent on the forkhead transcription factor FoxP3 (*22*). T_{regs} express high levels of CD25, glucocorticoid-induced TNFR (tumor necrosis factor receptor)–related protein (GITR), cytotoxic T lymphocyte antigen–4 (CTLA-4), and programmed cell death–1 (PD-1). T_{regs} secrete regulatory cytokines such as IL-10 that endow them with the capacity to maintain immune homeostasis and resolve IFN-γ–dependent T helper cell 1 (T_H1) responses (*23*). Previous studies have reported that T_{regs} accumulate in dystrophic muscle (*24*) and have shown that *FOXP3* mRNA is increased in muscle from osteopontin-deficient mdx mice, suggesting that their numbers or stability is partly regulated by osteopontin (*25*). Burzyn and colleagues recently demonstrated that T_{regs}, expressing high levels of amphiregulin and IL-10, accumulated during later stages of muscle repair and that depletion of CD25-expressing cells, including T_{regs}, in mdx mice exacerbated muscle injury (*26*). However, a specific examination of the functional role of T_{regs} in muscular dystrophy is still lacking.

In this investigation, we found that T_{regs} are elevated in human DMD/BMD and mouse mdx muscle and display an activated phenotype. We used a combination of loss-of-function methods that specifically

[1]Diabetes Center, University of California, San Francisco, San Francisco, CA 94143, USA. [2]Department of Neurology and Center for Duchenne Muscular Dystrophy, University of California, Los Angeles, Los Angeles, CA 90095, USA. [3]Institute for Infection Immunology, Twincore, Hannover 30625, Germany. [4]Molecular, Cellular, and Integrative Physiology Program, University of California, Los Angeles, Los Angeles, CA 90095, USA. [5]Department of Pathology, University of California, San Francisco, San Francisco, CA 94143, USA. [6]Department of Medicine, University of California, San Francisco, San Francisco, CA 94143, USA. *Corresponding author. E-mail: avillalta@diabetes.ucsf.edu

targeted T_{regs} to examine if T_{regs} regulate the pathogenesis and progression of muscular dystrophy. Histological and biochemical analysis of dystrophic muscle depleted of T_{regs} revealed an increase in immune cell infiltration and an enhanced type 1 inflammatory response, which resulted in exacerbated myofiber damage. The suppressive effect of T_{regs} on dystrophinopathy was further supported by the amelioration of muscle inflammation and injury in mdx mice treated with IL-2c. Collectively, these findings show that T_{regs} play a critical role in limiting muscle damage during muscular dystrophy by suppressing the development of type 1 inflammatory responses and demonstrate the potential clinical value of therapeutically targeting T_{regs} in DMD.

RESULTS

T_{regs} are elevated in the muscles of muscular dystrophy patients

The examination of muscle biopsies from control subjects and subjects with dystrophinopathy (table S1) by epifluorescence microscopy showed that T_{regs} were increased in DMD/BMD muscle biopsies compared to control muscle biopsies (Fig. 1). Necrotic lesions in dystrophic muscle were distinguished by $CD3^+$ T cell aggregates (Fig. 1D, green) containing $FoxP3^+$ cells (Fig. 1E, red) that were all $CD3^+$ (Fig. 1F); these features were largely absent in controls (Fig. 1, A to C). Quantification of lymphoid populations in DMD/BMD and control groups revealed a significant increase in the number of $CD3^+$ ($P < 0.05$) and $FoxP3^+$($P < 0.01$) cells in dystrophic muscle, but the frequency of $FoxP3^+$ cells among $CD3^+$ cells was not altered (Fig. 1, G to I, and table S2). Moreover, elevated numbers of $FoxP3^+$ cells coincided with increased IL-10 expression in DMD/BMD muscle compared to control muscle ($P < 0.05$) (Fig. 1J).

Muscle inflammation in mdx mice is associated with increased T_{regs}

Studies performed on the mdx mouse have shown that inflammation is a key pathological component contributing to the pathogenesis of muscular dystrophy. Thus, we used the mdx mouse model to study the capacity of T_{regs} to regulate muscle inflammation and injury during muscular dystrophy. Flow cytometry provided a sensitive and quantitative method to determine the cellular composition of the inflammatory infiltrate in mdx muscle (fig. S1A). We found that the total cellularity obtained from single-cell preparations of collagenase-digested muscle was increased in mdx mice relative to wild-type mice (fig. S1B), likely attributable to the increased proportion (fig. S1C) and absolute quantity (fig. S1D) of $CD45^+$ cells in mdx muscle. Moreover, the proportion of $Thy1^+$ cells was reduced at 4 weeks of age but higher at 12 weeks of age relative to age-matched controls (fig. S1E). The increased proportion of $Thy1^+$ cells in mdx mice is likely attributable to the reduced numbers of myeloid cells in muscle of 12-week-old mdx mice relative to 4-week-old mice and the relative increase in $CD4^+$ T cells during this time (*11*, *27*). The absolute number of $Thy1^+$ cells was increased in mdx mice at all ages examined relative to age-matched controls (fig. S1F).

Next, we examined the composition of $CD4^+$ T cells and found that the proportion of $CD45^+Thy1^+$ cells in mdx mice was increased at 12 weeks compared to age-matched controls and 4-week-old mdx mice but did not differ between 4-week-old mdx and wild-type mice

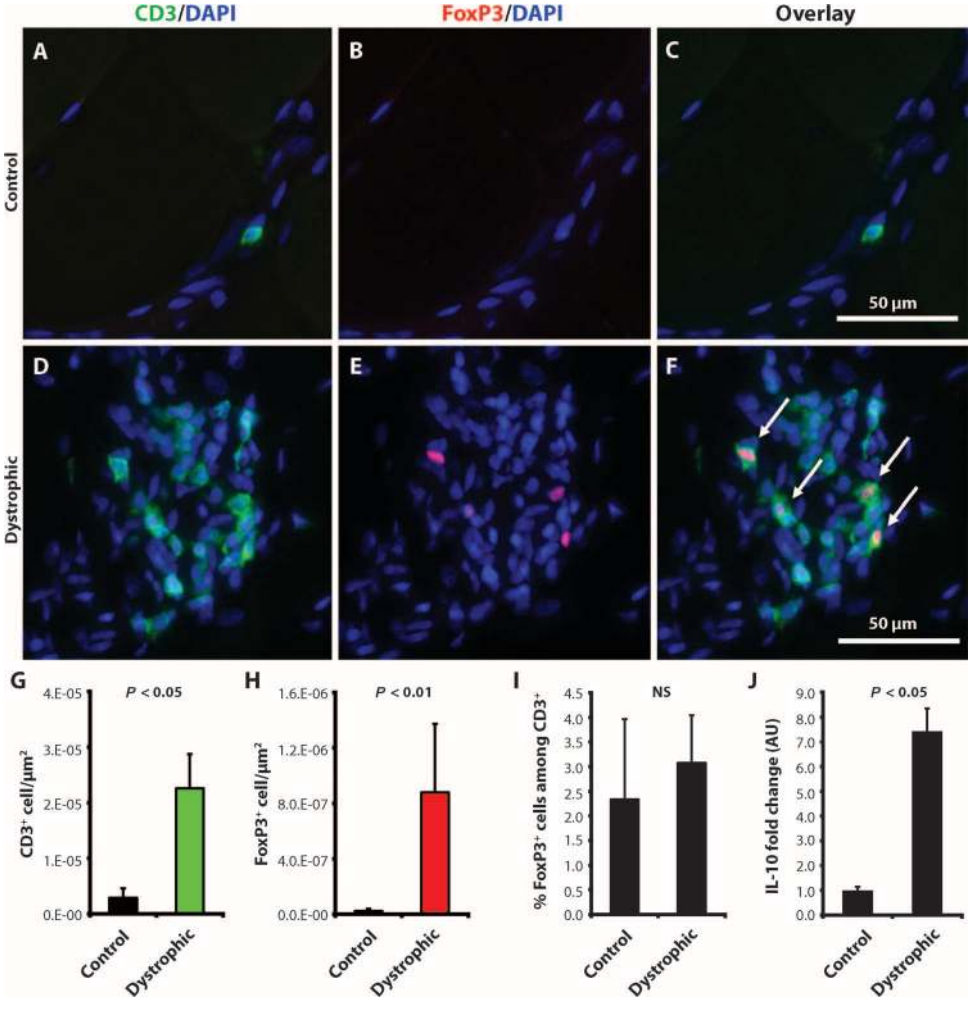

Fig. 1. T_{regs} are elevated in muscle of human subjects with DMD/BMD. (**A** to **F**) Immunofluorescence staining of CD3 (green, A and D) and FoxP3 (red, B and E) in control (A to C) and DMD (D to F) muscle sections. Overlaid images reveal that $FoxP3^+$ cells express CD3 (F, white arrows); nuclei were counterstained with 4′,6-diamidino-2-phenylindole (DAPI) (blue). (**G** and **H**) Quantification of the number of $CD3^+$ (G) and $FoxP3^+$ (H) cells per tissue sectional area. (**I**) Frequency of $FoxP3^+$ cells among $CD3^+$ cells. NS, not significant. (**J**) IL-10 mRNA in whole muscle was measured by reverse transcription quantitative polymerase chain reaction (RT-qPCR). Five and seven muscle samples were analyzed for the control and dystrophic groups, respectively. Statistical significance was determined by the nonparametric Mann-Whitney test.

(Fig. 2, A and B). However, the absolute number of $CD4^+$ T cells was increased in mdx mice at all ages examined relative to age-matched controls (Fig. 2C). An extremely rare population of $FoxP3^+$ T_{regs} was found in wild-type mouse muscle (Fig. 2, D to F). However, a substantial increase in the proportion (Fig. 2E) and absolute number (Fig. 2F) of T_{regs} was found in mdx mouse muscle at 4 and 12 weeks of age. In addition to splenomegaly and increased lymph node cellularity, we found that total $CD4^+$ T cells and $FoxP3^+$ T_{regs} were also elevated in the para-aortic lymph node (PaLN) of mdx mice (fig. S2).

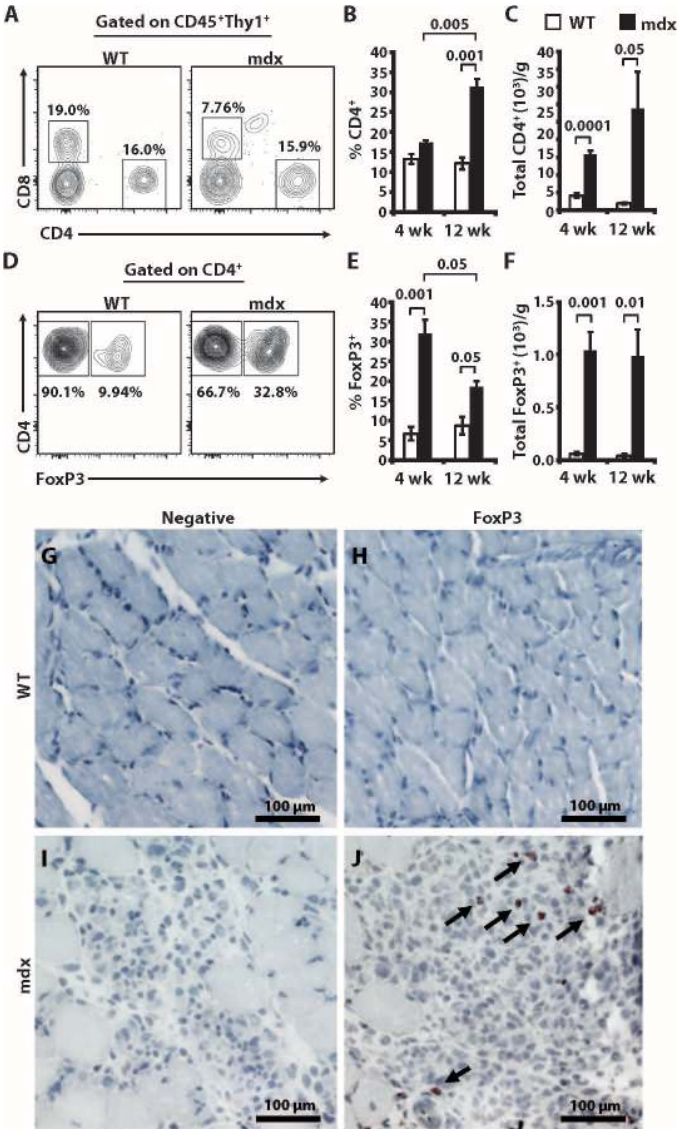

Fig. 2. T_{regs} are elevated in mdx mice. (**A** and **D**) Representative contour plots showing the frequency of $CD4^+$, $CD8^+$, and $FoxP3^+$ T cells in muscle. WT, wild type. (**B** and **C**) Frequency (B) and absolute number (C) of $CD4^+$ T cells normalized to muscle mass. (**E** and **F**) Frequency (E) and absolute number (F) of $FoxP3^+$ cells in WT and mdx muscle. The data are presented as a cumulative analysis of six independent experiments with four to five mice per group. The numerical values in (B), (C), (E), and (F) reflect the level of statistical significance determined by a two-tailed Student's *t* test. (**G** to **J**) Four-week-old WT (G and H) and mdx (I and J) muscles showing the distribution of $FoxP3^+$ cells. Shown are negative controls in which the FoxP3 antibody was omitted (G and I) and sections stained with anti-FoxP3 antibody (H and J). Black arrows in (J) highlight $FoxP3^+$ cells that reside in necrotic/inflammatory lesions in muscle.

T_{regs} are localized in muscle lesions

Next, we used histological techniques to examine the localization of T_{regs} in muscle to gain insights into the functional significance of these cells in the pathogenesis of muscular dystrophy. T_{regs} in wild-type muscle were so rare that they were not detected by immunohistochemical staining of frozen cross sections of wild-type quadriceps (Fig. 2H) or diaphragm (fig. S3B). In contrast, $FoxP3^+$ cells were found within inflamed, necrotic lesions in mdx quadriceps (black arrows in Fig. 2J) and diaphragm (fig. S3D). Muscle sections in which the anti-FoxP3 antibody was omitted during the staining procedure served as negative controls (Fig. 2, G and I, and fig. S3, A and C).

Muscle T_{regs} display an activated phenotype and express IL-10

Representative contour plots show that the frequencies of muscle T_{regs} expressing the activation markers killer cell lectin-like receptor subfamily G member 1 (KLRG1) and GITR or PD-1 were increased in mdx mouse muscle relative to wild-type muscle (Fig. 3A). Infrequent populations of $KLRG1^+GITR^+$ and $KLRG1^+PD\text{-}1^+$ T_{regs} were found in PaLN and were slightly increased in mdx mice at 4 weeks of age relative to age-matched control mice (Fig. 3, B and C). However, the frequencies of $KLRG1^+GITR^+$ and $KLRG1^+PD\text{-}1^+$ muscle T_{regs} were greatly increased relative to PaLN, with a greater increase in mdx muscle relative to wild-type muscle [Fig. 3, D ($P < 0.05$) and E ($P < 0.01$)]. Although PD-1 was not significantly increased, the expression of KLRG1 and GITR was increased in mdx muscle T_{regs} (Fig. 3, F to H). KLRG1 was not expressed on muscle conventional T cells (T_{convs}) (fig. S4); thus, we examined the frequencies of single-positive GITR and PD-1 muscle T_{convs}. We found that $GITR^+$ T_{convs} were elevated in mdx mice at all ages examined (fig. S4B) and $PD\text{-}1^+$ T_{convs} were elevated at 12 weeks (fig. S4C). Although GITR expression on mdx muscle T_{convs} was increased relative to age-matched controls, the expression was lower than that found on T_{regs} (fig. S4D). No difference in the expression of KLRG1 or PD-1 was observed between mdx and wild-type muscle T_{convs} (fig. S4, E and F).

Recently, T_{regs} accumulating in acutely injured muscle were shown to express high levels of IL-10 (*26*), a suppressive cytokine that was previously shown to reduce the pathology of muscular dystrophy in mdx mice (*20*). RT-qPCR analysis revealed that IL-10 was expressed by multiple immune cell subsets purified from mdx muscle by fluorescence-activated cell sorting (Fig. 3I). IL-10 was not expressed substantially in PaLN T_{regs} at 4 or 12 weeks of age in mdx mice when a large increase in IL-10 was detected in muscle T_{regs} (Fig. 3I).

Depletion of T_{regs} exacerbates muscle inflammation and injury in mdx mice

The increased number, activation, and localization of T_{regs} in dystrophic muscle suggest that they suppress myofiber injury due to the chronic muscle inflammation triggered by the mechanical frailty of dystrophin-deficient myofibers. Mdx mice were treated with a T_{reg}-depleting anti-CD25 antibody, clone PC61, to test this hypothesis (*28*). We began treatment at 3 weeks of age when disease onset occurred to prevent difficulties in interpreting the effect on T_{reg} depletion on dystrophinopathy because PC61 treatment in neonatal mice may cause multiorgan autoimmunity. Treated mdx mice were sacrificed at 6 weeks of age to allow

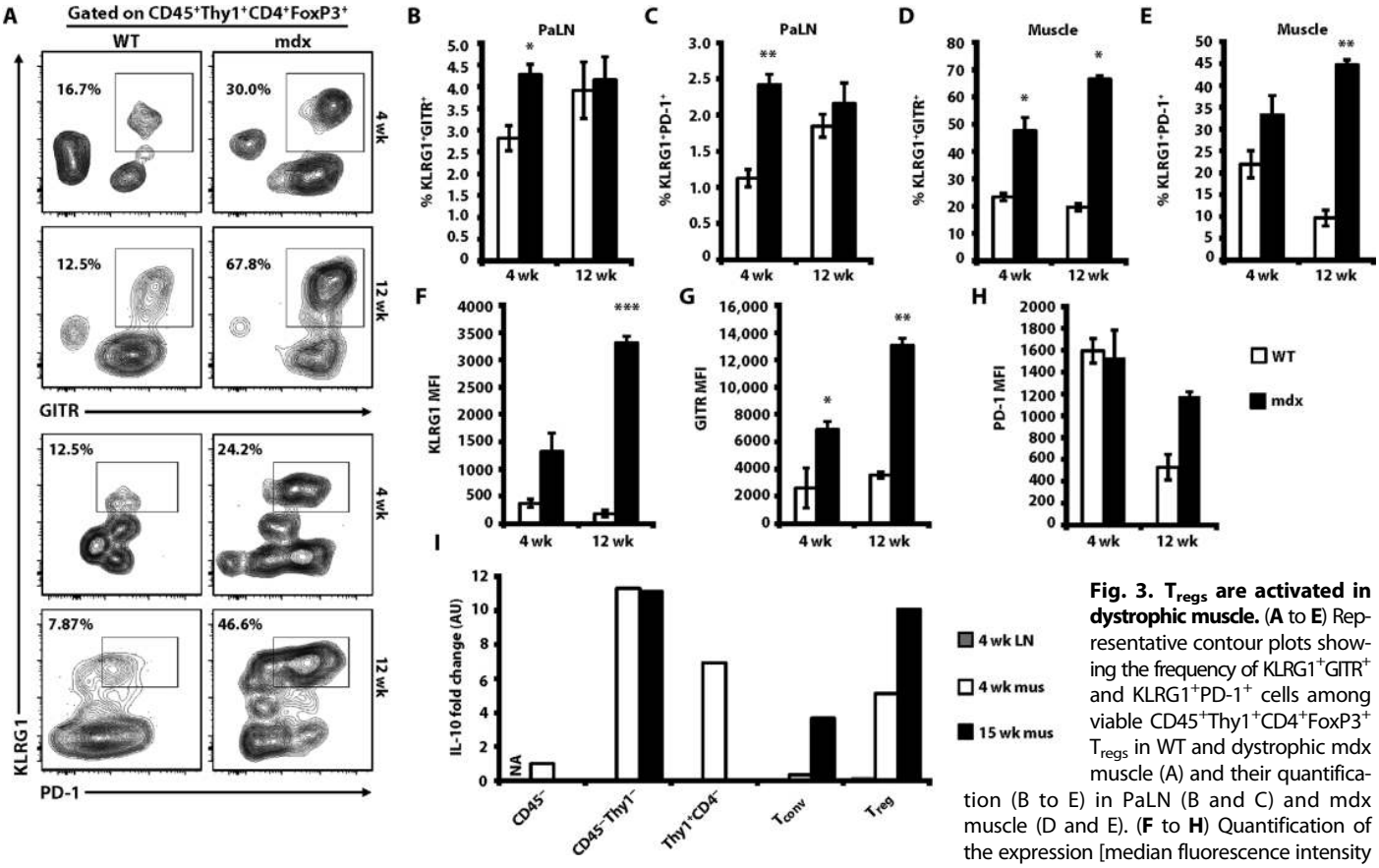

Fig. 3. T_{regs} are activated in dystrophic muscle. (**A** to **E**) Representative contour plots showing the frequency of KLRG1$^+$GITR$^+$ and KLRG1$^+$PD-1$^+$ cells among viable CD45$^+$Thy1$^+$CD4$^+$FoxP3$^+$ T_{regs} in WT and dystrophic mdx muscle (A) and their quantification (B to E) in PaLN (B and C) and mdx muscle (D and E). (**F** to **H**) Quantification of the expression [median fluorescence intensity (MFI)] of KLRG1 (F), GITR (G), and PD-1 (H) in muscle T_{regs}. Data reflect a cumulative analysis of seven independent experiments. Four-week-old WT mice; $n = 3$ (5 to 7 mice pooled per sample). Four-week-old mdx mice; $n = 8$ (1 mouse per sample). Twelve-week-old WT mice; $n = 2$ (3 to 4 mice per sample). Twelve-week-old mdx mice; $n = 3$ (1 mouse per sample). (**I**) Quantification of IL-10 expression by RT-qPCR in muscle cell populations sorted from 4- and 15-week-old mdx^{DEREG} mice. Data reflect a cumulative analysis of two independent experiments performed at 4 and 15 weeks of age. Five to six mice were pooled into one sample for each population, and age was analyzed. LN, pooled lymph nodes; mus, hindlimb muscles pooled from five to six mice. T_{conv}, CD45$^+$Thy1$^+$CD4$^+$FoxP3(GFP)$^-$ T cells; T_{reg}, CD45$^+$Thy1$^+$CD4$^+$FoxP3(GFP)$^+$ T cells. NA, not applicable. Statistical significance was determined by Student's *t* test with Welch correction: *$P < 0.05$, **$P < 0.01$, and ***$P < 0.001$.

sufficient time for the development of muscle injury and remodeling. As seen previously (*29*), PC61 treatment significantly decreased the proportion of CD4$^+$CD25$^+$ T cells (fig. S5A) and FoxP3$^+$ T_{regs} (fig. S5B) in mdx mice. A histological examination of quadriceps muscle sections revealed an increased inflammatory infiltrate in muscle of mdx mice treated with PC61 relative to control-treated mdx mice (Fig. 4, A and B). In addition, PC61 treatment increased the expression of IFN-γ and transforming growth factor–β (TGFβ) in mdx muscle (Fig. 4C), suggesting that T_{regs} or other CD25$^+$-expressing cells regulate the expression of these cytokines in dystrophic muscle. However, PC61 treatment did not influence the expression of T_H2, IL-10, or IL-17A cytokines. PC61 treatment increased the number of myofibers with accumulated albumin, indicating increased muscle injury after T_{reg} depletion (Fig. 4, D to F).

Given that PC61 may deplete non-T_{regs} that express CD25, the altered cytokine expression after PC61 treatment may not be due solely to the depletion of T_{regs}. Therefore, mdx mice were crossed with the DEREG mouse in which the FoxP3 promoter controls the expression of a green fluorescent protein (*GFP*)–diphtheria toxin receptor (*DTR*) transgene (*30*). This animal model (mdx^{DEREG}) facilitated the specific and acute ablation of lymph node (fig. S6A) and muscle T_{regs} (fig. S6B) in mdx mice after diphtheria toxin (DT) treatment. Consistent with previous studies (*31*), a rapid recovery of T_{reg} numbers was observed after DT treatment (black line, fig. S6, A and B), but a substantial proportion did not express the GFP-DTR fusion protein (gray line versus dashed line, fig. S6, A and B). Thus, the recovering T_{regs} could not be fully ablated by repeated treatment with DT.

On the 4th day after initiation of DT treatment, muscle (Fig. 4G, $P < 0.01$) and PaLN T_{regs} (fig. S6, C and D; $P < 0.0001$) were still significantly reduced, whereas the frequency of activated T_{convs} in muscle (Fig. 4H, $P < 0.05$) and PaLN (fig. S6D, $P < 0.001$) was increased. Similar to PC61-treated mdx mice, we found that IFN-γ was significantly increased in mdx^{DEREG} muscle that was depleted of T_{regs} (Fig. 4I, $P < 0.05$). Although a decrease in IL-5 was also seen, depletion of T_{regs} did not influence the expression of other T_H2, IL-10, or IL-17A cytokines. To define the cellular source of IFN-γ, we sorted bulk populations of myeloid (CD45$^+$Thy1$^-$) and lymphoid (CD45$^+$Thy1$^+$) cells and found that IFN-γ was predominantly confined to the lymphoid compartment in mdx mice (fig S6E). Intracellular cytokine staining of CD4$^+$ T cells revealed an increased

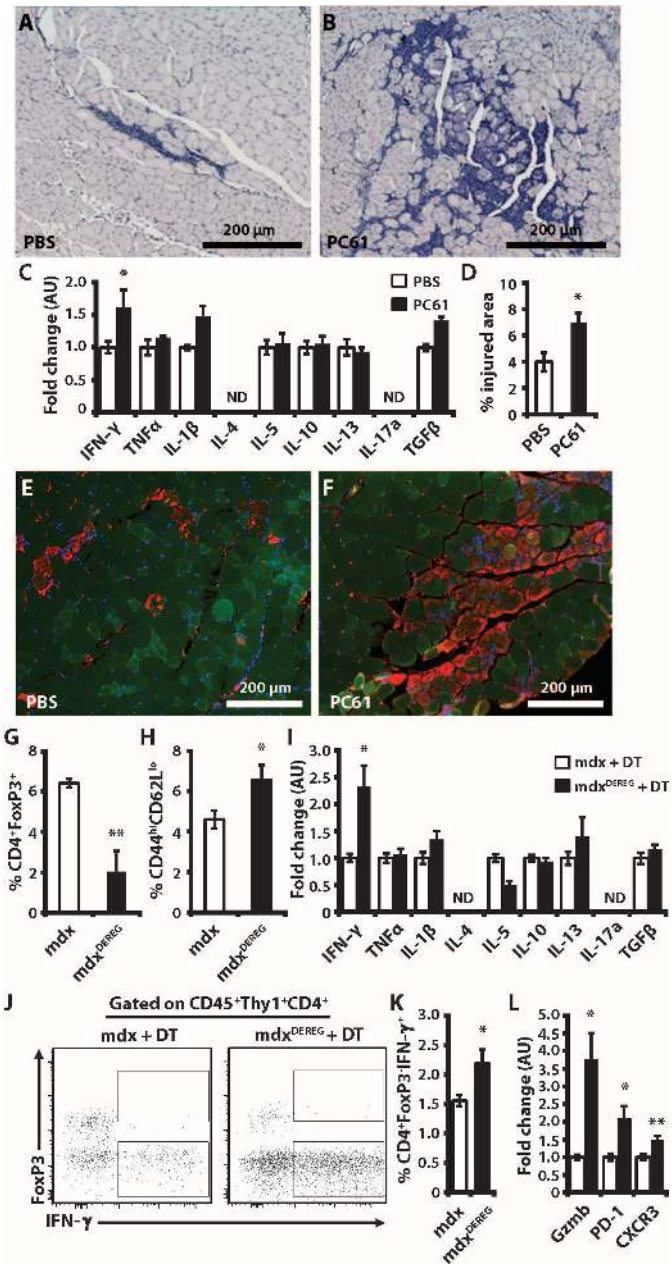

Fig. 4. T_{reg} depletion increases the IFN-γ response in muscle and exacerbates muscular dystrophy. (**A** to **B**) Hematoxylin-stained quadriceps muscle from 6-week-old control (A) and PC61-treated (B) mice. PBS, phosphate-buffered saline. (**C**) Expression of inflammatory cytokines in control- and PC61-treated mdx muscle. ND, not determined. (**D**) Muscle injury was quantified and expressed as the percent albumin-positive muscle area over total muscle area. Five to eight mice were used per group. (**E** and **F**) Representative images of quadriceps muscle from PC61-treated mdx mice (F) and control mice (E). Red, green, and blue stainings reveal albumin-positive muscle, total muscle, and nuclei, respectively. (**G** to **L**) Effect of T_{reg} depletion on muscle inflammation in mdx^{DEREG} mice. Five to seven mice were used per group. The frequency of $CD4^+FoxP3^+$ T_{regs} gated on $CD45^+Thy1^+$ (G) and of $CD44^{hi}CD62L^{lo}$T cells gated on $CD45^+Thy1^+CD4^+Foxp3^-$ (H). The expression of inflammatory cytokines was measured in whole muscle by RT-qPCR (I) and IFN-γ intracellular staining of muscle $CD45^+Thy1^-CD4^+$ T cells (J). Shown is the frequency of muscle $CD4^+FoxP3^-IFN\text{-}\gamma^+$ effector T cells (K). $n = 4$ to 5 per group; each sample represents the pooling of cells isolated from two mice. The expression of effector molecules associated with a T_H1 response measured by RT-qPCR (L). $n = 7$ to 9 per group. Statistical significance was determined by Student's t test: $^*P < 0.05$ and $^{**}P < 0.01$. Data are a cumulative analysis performed on two to three independent experiments.

frequency of muscle T_{convs} expressing IFN-γ (Fig. 4, J and K) and expression of genes up-regulated during a T_H1 response, namely, *Gzmb* (granzyme B), *PD1*, and *CXCR3* (Fig. 4L). The frequency of IL-17A–expressing muscle T_{convs} was not affected by T_{reg} ablation, suggesting that T_{regs} specifically suppressed type 1 inflammatory responses during muscular dystrophy (fig. S6F).

T_{regs} regulate macrophage activation in muscle

In addition to promoting M1 activation of proinflammatory macrophages that contribute to muscle injury (*19*), IFN-γ also induces the expression of programmed death–ligand 1 (PD-L1) (*32*). Thus, PD-L1 serves as a sensitive readout of IFN-γ–mediated M1 macrophage activation. We found discrete populations of M1 ($CD11b^+F4/80^+SiglecF^-Ly6c^+CD301^-$) and M2 ($CD11b^+F4/80^+SiglecF^-Ly6c^-CD301^+$) macrophages in muscle of mdx mice that harbored a *DTR* transgene at the 3′ end of the endogenous *FOXP3* locus ($mdx^{FoxP3.DTR\text{-}KI}$) (Fig. 5A). $Mdx^{FoxP3.DTR\text{-}KI}$ mice allowed for the chronic depletion of T_{regs} with repeated DT treatment without the rebound of T_{regs} observed in mdx^{DEREG} mice (fig. S7). The depletion of T_{regs} in $mdx^{FoxP3.DTR\text{-}KI}$ mice (~90% reduction) resulted indirectly in a significant increased expression of PD-L1 on M1 ($P < 0.05$) and M2 ($P < 0.001$) macrophages without affecting the proportion of either population in dystrophic muscle after an 11-day depletion period (Fig. 5, B, D, and E). Moreover, T_{reg} depletion significantly ($P < 0.05$) decreased the expression of the M2 activation marker CD206 on M2 macrophages but had no effect on M1 macrophages (Fig. 5, C, F, and G).

Therapeutic targeting of T_{regs} reduces muscle inflammation and injury in dystrophic mice

To assess the value of targeting T_{regs} as a potential treatment for DMD, we treated mdx mice with low-dose IL-2c that selectively increased T_{regs} in vivo (*33*). We found that IL-2c significantly ($P < 0.05$) increased the frequency of $FoxP3^+$ T_{regs} (Fig. 6, A and B) and the expression of IL-10 (Fig. 6C) in hindlimb muscles of mdx mice. We next used an $mdx.cox\text{-}2^{Luc/+}$ reporter mouse to assess the effect of IL-2c treatment on muscle inflammation. Although no difference in luciferase signal was detected at 4 and 5 weeks of age, a significant ($P < 0.05$) decrease in signal intensity was observed in exercised 6-week-old mdx mice treated with IL-2c (Fig. 6D). Representative heat map images of mice used for noninvasive imaging revealed a reduced luciferase signal in the hindlimb muscles of $mdx.cox\text{-}2^{Luc/+}$ mice treated with IL-2c, indicating that IL-2c treatment reduced muscle inflammation (Fig. 6E). The reduced inflammation in IL-2c–treated mice was accompanied by a decrease in serum creatine kinase concentrations, a serum biomarker of muscle injury (Fig. 6F). These results were further corroborated by the histological observation that IL-2c treatment decreased the proportion of myofibers in the diaphragm that incorporated serum albumin, indicating reduced muscle injury (Fig. 6, G and H).

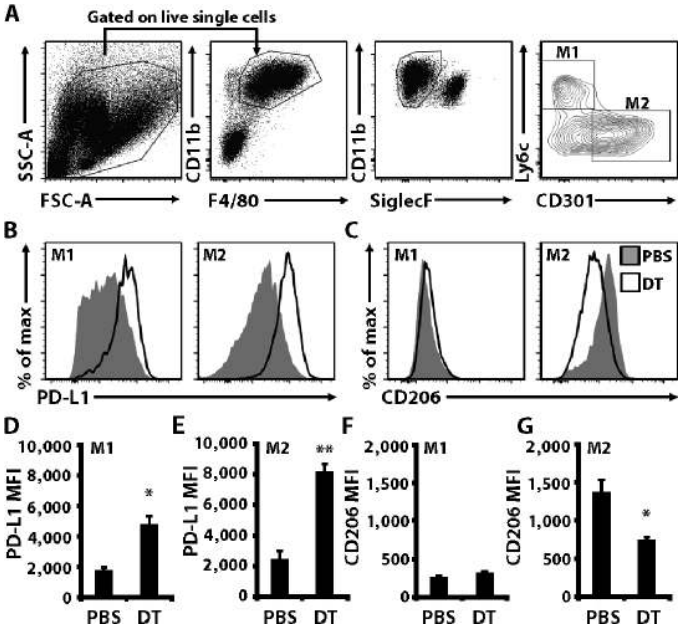

Fig. 5. T_{regs} regulate macrophage activation. (**A**) Representative dot plots showing the gating strategy used to define M1 and M2 macrophage populations. SSC-A, side scatter parameter; FSC-A, forward scatter parameter. (**B** and **C**) Representative histograms of PD-L1 (B) and CD206 (C) expression by macrophages in muscle. (**D** to **G**) Quantification of the MFI of PD-L1 (D and E) and CD206 (F and G) expression by M1 (D and F) and M2 (E and G) macrophages. Statistical significance was determined by Student's *t* test with Welch correction: $^{*}P < 0.05$ and $^{**}P < 0.01$. Data are representative of two independent experiments; $n = 3$ per group.

DISCUSSION

Our findings suggest that T_{regs} control the progression and pathophysiology of muscular dystrophy by restraining the development of a type 1 inflammatory response in muscle. We found that T_{regs} were elevated in muscle of human muscular dystrophy patients and mdx mice but largely absent in noninjured muscle, suggesting that downstream events after muscle injury are contributing factors that drive T_{reg} accumulation in dystrophic muscle. The localization of T_{regs} in necrotic lesions and their state of activation suggest that they actively suppress muscle inflammation. Indeed, we found that depletion of T_{regs} in mdx mice enhanced immune cell infiltration, muscle injury, and increased the expression of IFN-γ by muscle T_{convs} in mdx mice.

Previous investigations have shown that IFN-γ is chronically overexpressed in dystrophic muscle, increasing the M1/M2 macrophage ratio to promote myofiber injury (*18*, *19*). Moreover, the genetic deletion of IFN-γ in mdx mice reduces the severity of muscular dystrophy, further supporting a role for IFN-γ in the pathogenesis of muscular dystrophy (*18*). Our present findings that $Thy1^+$ lymphocytes, including $CD4^+$ effector T cells, are the predominant source of IFN-γ in dystrophic muscle, suggest that the chronic expression of IFN-γ is due to the expansion of these effector T cells and not myeloid cells such as macrophages. Our findings also indicate that muscle T_{regs} act centrally at the interface of muscle immunity and immune regulation by restraining the production of IFN-γ by $CD4^+$ effector T cells. Although we propose that the increased expression of IFN-γ after T_{reg} depletion is responsible for the enhanced M1 activation of macrophages, we cannot rule out the possibility that regulatory mechanisms that directly act on macrophages to suppress M1 activation are also lost. Indeed, we found that the depletion of T_{regs} decreased IL-5, a T_H2 cytokine that promotes the generation of eosinophils that are critical for the development of type 2 inflammation in injured muscle (*17*). However, whether the T_{reg}-mediated regulation of IL-5 has any effect on muscle eosinophilia or whether the type 2 inflammatory responses mediated by eosinophils contribute to M2 activation of macrophages in mdx mice remains to be determined.

T_{regs} control immune homeostasis and restrain inflammatory responses through a diverse number of molecular pathways, including the expression of the immune regulatory cytokine IL-10. For instance, during experimental autoimmune encephalomyelitis (EAE), a model of multiple sclerosis in which disease is cooperatively driven by T_H17 and T_H1 immunity, T_{regs} suppressed the severity of EAE by inhibiting the expression of IL-17 and IFN-γ in an IL-10–dependent manner (*34*). Transcriptional profiling of muscle T_{regs} isolated from acutely injured muscle revealed that muscle T_{regs} express exceptionally high levels of IL-10 compared to other lymphoid organ T_{regs} (*26*). Similarly, our findings that mdx muscle T_{regs} are a rich source of IL-10 suggest that the suppression of type 1 muscle inflammation by T_{regs} is IL-10–dependent. In support of this model, ablation of IL-10 in mdx mice has been shown to increase the severity of muscular dystrophy (*20*). Furthermore, in addition to increasing muscle T_{regs} and reducing muscle injury and inflammation, IL-2c treatment also increased the expression of IL-10 in mdx mouse muscle. However, an acute or partial depletion of T_{regs} in our study failed to show a change in IL-10 expression, suggesting that compensatory mechanisms might be at play or that additional regulatory mechanisms cooperate with IL-10 for the T_{reg}-mediated suppression of type 1 inflammation in muscle. Studies using IL-10 conditional knockout mdx mice in which IL-10 is specifically ablated in T_{regs} will aid in revealing the functional role of T_{reg}-derived IL-10 in the pathogenesis of muscular dystrophy.

In addition to their control of chronic inflammation, T_{regs} are critical in the maintenance of tolerance to self-antigens, as evidenced by catastrophic autoimmunity in mice and humans that lack FoxP3 (*35*–*37*). Although known autoantigens that drive muscle antigen–specific immune responses remain ill-defined, there is evidence that clonal expansion of autoreactive T cells in mdx mice and DMD patients does occur. In studies examining the pathogenic role of osteopontin in mdx mice, investigators found an enrichment of $V\beta8.1/8.2^+$ T cells in muscle (*25*), suggesting an oligoclonal expansion of T cells in response to presentation of muscle antigens after injury. In humans, sequencing of the complementarity-determining region 3 of the T cell receptor Vβ2 chain from DMD muscle biopsy revealed a conserved rearrangement, indicating that a common antigen within these patients was also driving a muscle antigen–specific immune response (*38*). Our observation that muscle $CD4^+$ T cells are activated in mdx mouse muscle is in agreement with the hypothesis that muscle antigens released after injury promote the activation and effector function of muscle T cells. In this regard, T_{regs} are likely to prevent muscle autoimmunity and restrain inflammation during the course of injury and antigen release.

In addition to self-antigens that promote immunity, the concern about autoreactive T cell responses also extends to dystrophin gene therapy, which introduces a neo-antigen that may be immunogenic. A recent study showed that a sizable proportion of DMD patients have a preexisting pool of dystrophin-reactive T cells (*39*). Moreover,

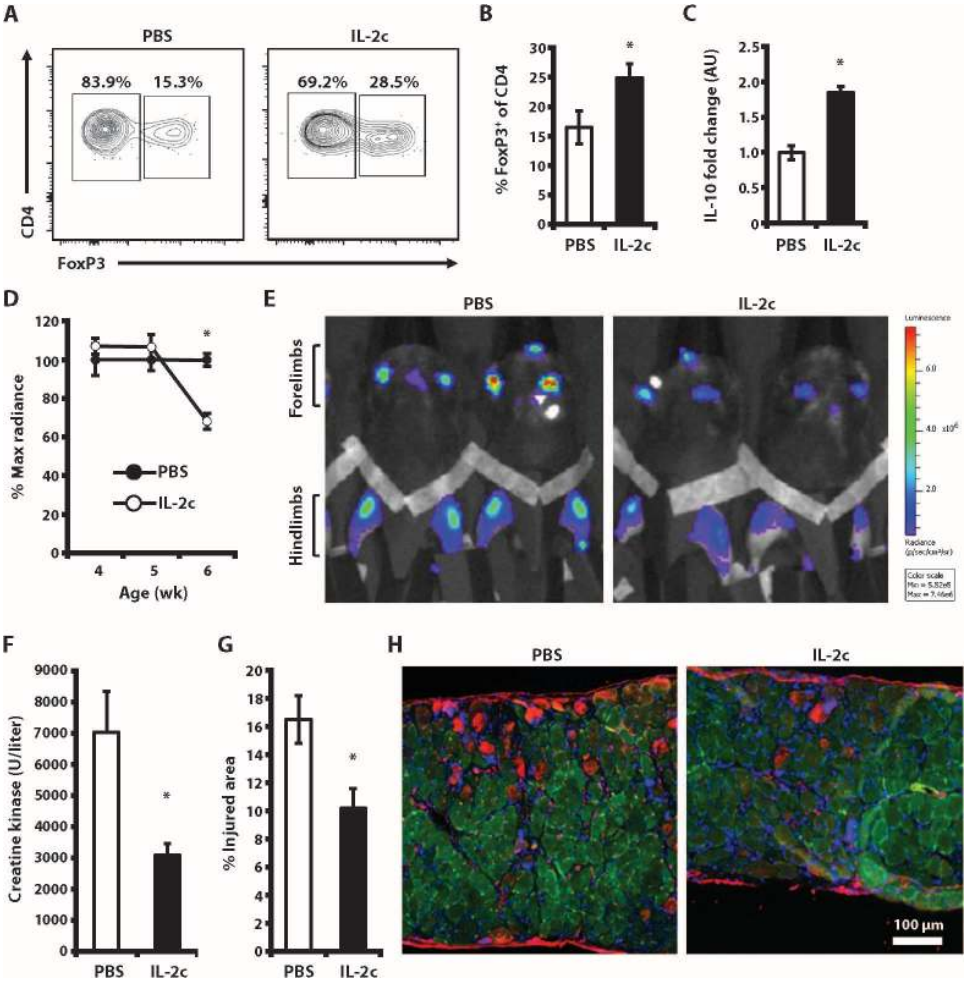

Fig. 6. IL-2 complexes augment muscle T_{regs} in vivo and ameliorate muscular dystrophy. (**A**) Representative contour plots showing the proportion of FoxP3$^+$ T_{regs} (gated on viable SSC^{lo}FSC^{lo}CD45$^+$Thy1$^+$CD4$^+$ T cells) in IL-2c–treated and control mdx mouse muscle. (**B**) Frequency of muscle T_{regs} in mdx mice treated with IL-2c. (**C**) Expression of IL-10 mRNA in quadriceps muscle of control and IL-2c–treated mdx mice. Data are representative of two independent experiments. (**D**) Quantification of the % max radiance over time after IL-2c treatment. (**E**) Representative whole-body heat map images of IL-2c–treated and control mdx.cox-2$^{Luc/+}$ mice, showing pseudocolor IVIS bioluminescence signatures over shaved forelimbs and hindlimbs. (**F**) Serum creatine kinase activity in IL-2c–treated and control mice. (**G**) Injured muscle area of IL-2c–treated and control mice expressed as a percentage of the total muscle area. (**H**) Representative muscle sections showing albumin-positive injured myofibers (red) and the total muscle area (green). Nuclei were counterstained with DAPI (blue). The data are representative of four to seven mice per group performed over three independent experiments. Statistical significance was determined by Student's *t* test: *$P < 0.05$.

a recent dystrophin gene therapy trial performed in a small number of patients revealed that a subset developed dystrophin-specific T cell responses (*40*). These preliminary observations together with the concern of unwanted side effects associated with chronic glucocorticoid therapy have prompted recent interest in developing immunotherapies that not only mitigate inflammation but also suppress dystrophin immunity (*41*). In this regard, our data implicate T_{regs} or T_{reg}-boosting agents as potential therapies that may be used in conjunction with gene therapy as an alternative approach to limit dystrophin immunity while limiting side effects associated with glucocorticoids. Further studies will be required to fully address the significance of the generation of dystrophin immunity during gene therapy, along with studies aimed at examining the capacity of T_{regs} to suppress dystrophin immunity during gene therapy.

The molecular attributes of muscle T_{regs} suggest that their function extends beyond mere regulation of muscle immunity to modulation of tissue repair and remodeling processes. Burzyn *et al.* (*26*) recently reported that muscle T_{regs} express amphiregulin and that treatment of injured muscle with exogenous amphiregulin improved muscle regeneration, possibly by promoting satellite cell differentiation. Moreover, they showed that the depletion of T_{regs} during acute muscle injury not only impaired muscle healing but also increased fibrosis. We found that chronic depletion of T_{regs} with PC61 treatment increased the levels of the profibrotic factor TGFβ, further supporting a relationship between T_{regs} and the negative regulation of fibrosis. However, it remains to be defined whether amphiregulin negatively regulates the expression of TGFβ or whether other factors are responsible for this regulation. In this regard, recent studies have shown that osteopontin deficiency in mdx mice increased *FOXP3* mRNA in muscle but reduced *TGFβ1* and muscle fibrosis (*25*). Moreover, we have found that T_{regs} make an antifibrotic factor, relaxin-3 (*42*), which is overexpressed in mdx mice as T_{reg} numbers increase in mdx muscle. Considering that relaxin-3 also has anti-inflammatory properties, it is interesting to speculate that in addition to reducing fibrosis, relaxin-3 may suppress muscle inflammation independently or cooperatively with IL-10. It is important to note that the depletion of T_{regs} in the mdx^{DEREG} mouse did not increase TGFβ, which may be explained by the acute nature of the T_{reg} depletion in this model. Alternatively, the increased TGFβ and decreased IL-5 in PC61-treated mice might be attributed to the depletion of a non-T_{reg} cell population that expresses CD25.

Collectively, our data and previously reported findings support a model in which as yet unidentified signals arising from muscle injury recruit and expand muscle T_{regs} that restrain type 1 muscle inflammation and secrete factors that enhance muscle regeneration. Specifically, T_{regs} suppress the expression of IFN-γ by CD4$^+$ T cells and the subsequent activation of muscle injury–promoting M1 macrophages. IL-10 is a candidate molecule that may mediate the suppressive function of muscle T_{regs} during muscular dystrophy, but the lack of change in IL-10 after T_{reg} depletion suggests that alternative mechanisms are also involved. Because IFN-γ can directly inhibit myoblast proliferation

(*43*), T_{regs} also participate in muscle regeneration by inhibiting the antimyogenic activity of IFN-γ expressed by T_{convs} and through secretion of factors, such as amphiregulin, that act directly on myogenic cells. Considering that fibrosis is a prominent feature of DMD that is exacerbated by T_{reg} depletion, further research is warranted to understand the relationship between T_{regs} and the development of fibrosis during muscular dystrophy, and how this axis cooperates with amphiregulin, or other regenerative factors (that is, relaxin-3), to promote muscle regeneration. As mentioned above, human DMD patients and mdx mice, although sharing many pathological features, differ in the rate of disease progression and the severity of muscle deterioration and loss of muscle function. It is interesting to speculate that such variations in clinical presentation may be due to differences in the phenotypic character, functional state, or altered recruitment kinetics of muscle T_{regs} in human versus mouse. In summary, our studies and those reported recently by other investigators (*26*) reveal the therapeutic potential of targeting T_{regs} in muscular dystrophy and other muscle disorders.

MATERIALS AND METHODS

Study design

We aimed to study the number and function of immune cells within the tissue of humans with DMD and BMD. To identify dystrophinopathy samples for histologic studies, we performed a computerized search of the University of California, San Francisco (UCSF) neuropathology case database spanning the interval between 2002 and 2013; five muscle biopsies for which frozen tissue was available were included in the dystrophinopathy group. Two additional samples were analyzed by collaborators at University of California, Los Angeles (UCLA) (M.J.S.). For the control group, patients were biopsied because of clinical suspicion for some muscle diseases (that is, necrotizing myopathy and inflammatory myopathy), but blinded sampling yielded uninvolved/normal tissue. Group assignment was based on histologic features of dystrophinopathy alone, and no attempt was made to match participants by age, sex, or other demographic variables (table S1). Immunohistochemical and immunofluorescence staining of frozen cross sections was performed as previously described (*19*). Anti-human FoxP3 antibody (eBioscience) was applied to muscle sections overnight at 4°C. Alexa 555–conjugated secondary antibodies were used to visualize primary antibody–specific staining. Nuclei were counterstained with DAPI. Bright-field and epifluorescent images were captured with a Zeiss Axio Imager microscope or Zeiss ApoTome microscope, respectively. The morphological features of muscular dystrophy were assessed by staining formalin-fixed cross sections of mdx muscle with hematoxylin. Representative images of hematoxylin and eosin–stained muscle sections showing the severity of muscle pathology in patients with muscular dystrophy and controls are provided (fig. S8). The study design was reviewed and approved by the UCSF Committee on Human Research (CHR). For studies on archival muscle biopsy tissue, the informed consent requirement was waived by the CHR given a minimal potential for harm to study participants. No individually identifiable patient data are presented.

We aimed to study the number and function of immune cells within the tissue of mice with muscular dystrophy, as well as the functional consequence of T_{reg} manipulation. Thus, we set up a number of animal studies designed to evaluate T_{regs} in muscle tissues and study inflammation during disease progression in mdx versus control mice. To accomplish this, C57BL/6, C57BL/10, and B6.129 (Cg)-FoxP3$^{tm3(DTR/GDP)Ayr}$/J mice (purchased from The Jackson Laboratory) and DEREG mice (*30*), provided by T.S., were crossed with mdx mice (C57BL/10ScSn-Dmd^{mdx}/J, The Jackson Laboratory). Mdx mice containing a *luciferase* transgene transcriptionally controlled by the *cyclooxygenase-2* (*cox-2*) promoter were created by crossing the mdx mouse with the *cox-2/luciferase* knock-in mouse created by H. Herschman, which was backcrossed a minimum of five times to C57BL/6 background (*44*). F_1 heterozygous littermates were intercrossed to obtain *cox-2/luciferase* heterozygous and *dystrophin*-null mice (mdx.cox-2$^{Luc/+}$). The *cox-2/luciferase* knock-in allele was always maintained in the heterozygous state. All mice were bred in a pathogen-free facility at UCSF, and animal experiments were approved by the Institutional Animal Care and Use Committee of UCSF or UCLA.

Mouse histology

Immunohistochemical and immunofluorescence staining of frozen cross sections was performed as previously described (*19*). Briefly, anti-mouse FoxP3 (eBioscience) or anti-human serum albumin antibody (AbD Serotec) was applied to muscle sections overnight at 4°C. Mouse FoxP3 staining was visualized with secondary immunoreagents and 3-amino-9-ethylcarbazole peroxidase substrate (Vector Laboratories). Alexa 555–conjugated secondary antibodies were used to visualize primary antibody–specific staining. Nuclei were counterstained with DAPI. Bright-field and epifluorescent images were captured with a Zeiss Axio Imager microscope or Zeiss ApoTome microscope, respectively. The morphological features of muscular dystrophy were assessed by staining formalin-fixed cross sections of mdx muscle with hematoxylin.

In vivo T_{reg} ablation

$CD25^+$ T_{regs} were depleted in mdx mice, using a modification of an in vivo depletion protocol previously described (*29*). Three-week-old mdx mice were injected twice with 250 μg of an anti-CD25 antibody (clone PC61). Mice were sacrificed, and muscles were harvested at 6 weeks of age for histological examination to assess the effect of T_{reg} depletion on muscular dystrophy. To specially deplete T_{regs}, mdx mice were crossed to the DEREG mouse or the FoxP3.DTR-GFP knock-in (FoxP3.DTR-KI) mouse. T_{regs} in 4- to 5-week-old mdx^{DEREG} mice were depleted with two consecutive daily intraperitoneal injections of DT (40 μg/kg), and the mice were sacrificed at day 4. T_{regs} were depleted in 3-week-old mdx$^{FoxP3.DTR-KI}$ mice by injecting DT every other day over an 11-day period. No mortalities or signs of overt morbidity (that is, dehydration, lethargy, or ruffled coat) were observed in mdx$^{FoxP3.DTR-KI}$ in the time frame and dosage used in these experiments. A small loss of body mass was detected as reported previously (*45*).

Muscle injury assays

Injured fibers that allow the diffusion and accumulation of serum proteins in their cytoplasm were identified in cross sections of quadriceps muscles by immunostaining with anti-albumin (AbD Serotec), followed by an Alexa 555–conjugated secondary antibody. Imaging was performed on a Zeiss ApoTome microscope. The total and injured muscle area was measured with MetaMorph automation and image analysis software (Molecular Devices).

IL-2c treatment of mdx mice

The treatment of mdx mice with IL-2/anti–IL-2 complexes was initiated at 2 weeks of age. Three doses were administered intraperitoneally every other day during the first week of treatment. Each dose consisted of 5.0 μg of recombinant mouse IL-2 (eBioscience) preincubated with 0.5 μg

of anti–IL-2 antibody (clone JES6-1A12, R&D Systems) for 15 min at 37°C. Mice were sacrificed at 6 weeks of age, and muscles and serum samples were collected for analysis.

In vivo bioluminescent imaging

To assess inflammation noninvasively, optical imaging (IVIS, Xenogen) was used to assess bioluminescence activity in IL-2c–treated and untreated mdx.cox-2$^{Luc/+}$ mice on the basis of the observation that immune cells express cox-2 upon activation. Mice were imaged at 4, 5, and 6 weeks of age. Because the luciferase signal in mdx.cox-2$^{Luc/+}$ mice was below the level of detection in rested animals, mice were exercised on a downhill treadmill at 19 m/min for 20 min and then imaged 2 days after exercise. Luciferase activity was then detected. For imaging, mice were weighed and anesthetized with 2% isoflorane, and limbs were shaved and injected intraperitoneally with D-luciferin (125 mg/kg). Mice were placed in a temperature-controlled chamber, ventral side up, within the IVIS imaging unit, and images were acquired with 1-min scans using medium binning at 15-, 20-, 25-, and 30-min time points. Living Image 4.0 software was used for the post-acquisition analysis of bioluminescence activity measured in photons and expressed in max radiance. Bioluminescence measurements of the hindlimbs were averaged together for each animal for statistical analysis.

Serum creatine kinase

To assess muscle membrane integrity, serum creatine kinase levels were assessed using a Creatine Kinase kit (Sekisui Diagnostics P.E.I. Inc.). Blood was collected via retro-orbital bleeding. Serum was isolated and immediately frozen at –80°C.

Statistical analysis

Statistical analyses were performed using GraphPad Prism version 5.01. Statistical comparisons between two groups were performed using an unpaired two-tailed Student's *t* test or a nonparametric Mann-Whitney test. Comparisons between multiples groups were performed by one-way or two-way analysis of variance, followed by a post hoc Bonferroni test to determine significance of differences between two groups. Values of $P \leq 0.05$ were considered significant.

SUPPLEMENTARY MATERIALS

www.sciencetranslationalmedicine.org/cgi/content/full/6/258/258ra142/DC1
Materials and Methods
Fig. S1. Increased leukocytes in mdx dystrophic muscle.
Fig. S2. Splenomegaly, lymphadenopathy, and increased cellularity in mdx mice.
Fig. S3. T_{regs} are elevated in mdx diaphragm muscle.
Fig. S4. T_{convs} are activated in dystrophic muscle.
Fig. S5. Anti-CD25 antibody-mediated depletion of T_{regs} in mdx mice.
Fig. S6. Specific ablation of T_{regs} in mdx^{DEREG} mice.
Fig. S7. Sustained T_{reg} ablation in mdx$^{FoxP3.DTR-KI}$ mice.
Fig. S8. The histological features of control and dystrophic muscle biopsies.
Table S1. Characteristics of the control and DMD/BMD patients used for histological examination.
Table S2. T cell counts in human patients.

REFERENCES AND NOTES

1. E. P. Hoffman, R. H. Brown Jr., L. M. Kunkel, Dystrophin: The protein product of the Duchenne muscular dystrophy locus. *Cell* **51**, 919–928 (1987).
2. M. Koenig, E. P. Hoffman, C. J. Bertelson, A. P. Monaco, C. Feener, L. M. Kunkel, Complete cloning of the Duchenne muscular dystrophy (DMD) cDNA and preliminary genomic organization of the DMD gene in normal and affected individuals. *Cell* **50**, 509–517 (1987).
3. A. P. Monaco, C. J. Bertelson, S. Liechti-Gallati, H. Moser, L. M. Kunkel, An explanation for the phenotypic differences between patients bearing partial deletions of the DMD locus. *Genomics* **2**, 90–95 (1988).
4. G. Bulfield, W. G. Siller, P. A. Wight, K. J. Moore, X chromosome-linked muscular dystrophy (*mdx*) in the mouse. *Proc. Natl. Acad. Sci. U.S.A.* **81**, 1189–1192 (1984).
5. T. A. Rando, Role of nitric oxide in the pathogenesis of muscular dystrophies: A "two hit" hypothesis of the cause of muscle necrosis. *Microsc. Res. Tech.* **55**, 223–235 (2001).
6. J. G. Tidball, M. Wehling-Henricks, Damage and inflammation in muscular dystrophy: Potential implications and relationships with autoimmune myositis. *Curr. Opin. Rheumatol.* **17**, 707–713 (2005).
7. D. G. Allen, B. T. Zhang, N. P. Whitehead, Stretch-induced membrane damage in muscle: Comparison of wild-type and *mdx* mice. *Adv. Exp. Med. Biol.* **682**, 297–313 (2010).
8. M. J. Spencer, J. G. Tidball, Do immune cells promote the pathology of dystrophin-deficient myopathies? *Neuromuscul. Disord.* **11**, 556–564 (2001).
9. B. Cai, M. J. Spencer, G. Nakamura, L. Tseng-Ong, J. G. Tidball, Eosinophilia of dystrophin-deficient muscle is promoted by perforin-mediated cytotoxicity by T cell effectors. *Am. J. Pathol.* **156**, 1789–1796 (2000).
10. M. J. Spencer, E. Montecino-Rodriguez, K. Dorshkind, J. G. Tidball, Helper (CD4$^+$) and cytotoxic (CD8$^+$) T cells promote the pathology of dystrophin-deficient muscle. *Clin. Immunol.* **98**, 235–243 (2001).
11. M. Wehling, M. J. Spencer, J. G. Tidball, A nitric oxide synthase transgene ameliorates muscular dystrophy in mdx mice. *J. Cell Biol.* **155**, 123–131 (2001).
12. S. Hodgetts, H. Radley, M. Davies, M. D. Grounds, Reduced necrosis of dystrophic muscle by depletion of host neutrophils, or blocking TNFα function with Etanercept in mdx mice. *Neuromuscul. Disord.* **16**, 591–602 (2006).
13. A. Y. Manzur, T. Kuntzer, M. Pike, A. Swan, Glucocorticoid corticosteroids for Duchenne muscular dystrophy. *Cochrane Database Syst. Rev.*, CD003725 (2008).
14. M. Wehling-Henricks, J. J. Lee, J. G. Tidball, Prednisolone decreases cellular adhesion molecules required for inflammatory cell infiltration in dystrophin-deficient skeletal muscle. *Neuromuscul. Disord.* **14**, 483–490 (2004).
15. R. M. Keeling, P. T. Golumbek, E. M. Streif, A. M. Connolly, Weekly oral prednisolone improves survival and strength in male *mdx* mice. *Muscle Nerve* **35**, 43–48 (2007).
16. J. G. Tidball, S. A. Villalta, Regulatory interactions between muscle and the immune system during muscle regeneration. *Am. J. Physiol. Regul. Integr. Comp. Physiol.* **298**, R1173–R1187 (2010).
17. J. E. Heredia, L. Mukundan, F. M. Chen, A. A. Mueller, R. C. Deo, R. M. Locksley, T. A. Rando, A. Chawla, Type 2 innate signals stimulate fibro/adipogenic progenitors to facilitate muscle regeneration. *Cell* **153**, 376–388 (2013).
18. S. A. Villalta, B. Deng, C. Rinaldi, M. Wehling-Henricks, J. G. Tidball, IFN-γ promotes muscle damage in the *mdx* mouse model of Duchenne muscular dystrophy by suppressing M2 macrophage activation and inhibiting muscle cell proliferation. *J. Immunol.* **187**, 5419–5428 (2011).
19. S. A. Villalta, H. X. Nguyen, B. Deng, T. Gotoh, J. G. Tidball, Shifts in macrophage phenotypes and macrophage competition for arginine metabolism affect the severity of muscle pathology in muscular dystrophy. *Hum. Mol. Genet.* **18**, 482–496 (2009).
20. S. A. Villalta, C. Rinaldi, B. Deng, G. Liu, B. Fedor, J. G. Tidball, Interleukin-10 reduces the pathology of *mdx* muscular dystrophy by deactivating M1 macrophages and modulating macrophage phenotype. *Hum. Mol. Genet.* **20**, 790–805 (2011).
21. M. Cheng, M. H. Nguyen, G. Fantuzzi, T. J. Koh, Endogenous interferon-γ is required for efficient skeletal muscle regeneration. *Am. J. Physiol. Cell Physiol.* **294**, C1183–C1191 (2008).
22. S. Z. Josefowicz, L. F. Lu, A. Y. Rudensky, Regulatory T cells: Mechanisms of differentiation and function. *Annu. Rev. Immunol.* **30**, 531–564 (2012).
23. M. A. Koch, G. Tucker-Heard, N. R. Perdue, J. R. Killebrew, K. B. Urdahl, D. J. Campbell, The transcription factor T-bet controls regulatory T cell homeostasis and function during type 1 inflammation. *Nat. Immunol.* **10**, 595–602 (2009).
24. S. Eghtesad, S. Jhunjhunwala, S. R. Little, P. R. Clemens, Rapamycin ameliorates dystrophic phenotype in *mdx* mouse skeletal muscle. *Mol. Med.* **17**, 917–924 (2011).
25. S. A. Vetrone, E. Montecino-Rodriguez, E. Kudryashova, I. Kramerova, E. P. Hoffman, S. D. Liu, M. C. Miceli, M. J. Spencer, Osteopontin promotes fibrosis in dystrophic mouse muscle by modulating immune cell subsets and intramuscular TGF-β. *J. Clin. Invest.* **119**, 1583–1594 (2009).
26. D. Burzyn, W. Kuswanto, D. Kolodin, J. L. Shadrach, M. Cerletti, Y. Jang, E. Sefik, T. G. Tan, A. J. Wagers, C. Benoist, D. Mathis, A special population of regulatory T cells potentiates muscle repair. *Cell* **155**, 1282–1295 (2013).
27. M. J. Spencer, C. M. Walsh, K. A. Dorshkind, E. M. Rodriguez, J. G. Tidball, Myonuclear apoptosis in dystrophic mdx muscle occurs by perforin-mediated cytotoxicity. *J. Clin. Invest.* **99**, 2745–2751 (1997).
28. O. Taguchi, T. Takahashi, Administration of anti-interleukin-2 receptor α antibody in vivo induces localized autoimmune disease. *Eur. J. Immunol.* **26**, 1608–1612 (1996).
29. Y. Y. Setiady, J. A. Coccia, P. U. Park, In vivo depletion of CD4$^+$FOXP3$^+$ Treg cells by the PC61 anti-CD25 monoclonal antibody is mediated by FcγRIII$^+$ phagocytes. *Eur. J. Immunol.* **40**, 780–786 (2010).

30. K. Lahl, C. Loddenkemper, C. Drouin, J. Freyer, J. Arnason, G. Eberl, A. Hamann, H. Wagner, J. Huehn, T. Sparwasser, Selective depletion of Foxp3$^+$ regulatory T cells induces a scurfy-like disease. *J. Exp. Med.* **204**, 57–63 (2007).
31. K. Lahl, T. Sparwasser, In vivo depletion of FoxP3$^+$ Tregs using the DEREG mouse model. *Methods Mol. Biol.* **707**, 157–172 (2011).
32. P. Loke, J. P. Allison, PD-L1 and PD-L2 are differentially regulated by Th1 and Th2 cells. *Proc. Natl. Acad. Sci. U. S. A.* **100**, 5336–5341 (2003).
33. O. Boyman, M. Kovar, M. P. Rubinstein, C. D. Surh, J. Sprent, Selective stimulation of T cell subsets with antibody-cytokine immune complexes. *Science* **311**, 1924–1927 (2006).
34. X. Zhang, D. N. Koldzic, L. Izikson, J. Reddy, R. F. Nazareno, S. Sakaguchi, V. K. Kuchroo, H. L. Weiner, IL-10 is involved in the suppression of experimental autoimmune encephalomyelitis by CD25$^+$CD4$^+$ regulatory T cells. *Int. Immunol.* **16**, 249–256 (2004).
35. J. M. Kim, J. P. Rasmussen, A. Y. Rudensky, Regulatory T cells prevent catastrophic autoimmunity throughout the lifespan of mice. *Nat. Immunol.* **8**, 191–197 (2007).
36. C. L. Bennett, J. Christie, F. Ramsdell, M. E. Brunkow, P. J. Ferguson, L. Whitesell, T. E. Kelly, F. T. Saulsbury, P. F. Chance, H. D. Ochs, The immune dysregulation, polyendocrinopathy, enteropathy, X-linked syndrome (IPEX) is caused by mutations of *FOXP3*. *Nat. Genet.* **27**, 20–21 (2001).
37. R. S. Wildin, F. Ramsdell, J. Peake, F. Faravelli, J. L. Casanova, N. Buist, E. Levy-Lahad, M. Mazzella, O. Goulet, L. Perroni, F. D. Bricarelli, G. Byrne, M. McEuen, S. Proll, M. Appleby, M. E. Brunkow, X-linked neonatal diabetes mellitus, enteropathy and endocrinopathy syndrome is the human equivalent of mouse scurfy. *Nat. Genet.* **27**, 18–20 (2001).
38. E. Gussoni, G. K. Pavlath, R. G. Miller, M. A. Panzara, M. Powell, H. M. Blau, L. Steinman, Specific T cell receptor gene rearrangements at the site of muscle degeneration in Duchenne muscular dystrophy. *J. Immunol.* **153**, 4798–4805 (1994).
39. K. M. Flanigan, K. Campbell, L. Viollet, W. Wang, A. M. Gomez, C. M. Walker, J. R. Mendell, Anti-dystrophin T cell responses in Duchenne muscular dystrophy: Prevalence and a glucocorticoid treatment effect. *Hum. Gene Ther.* **24**, 797–806 (2013).
40. J. R. Mendell, K. Campbell, L. Rodino-Klapac, Z. Sahenk, C. Shilling, S. Lewis, D. Bowles, S. Gray, C. Li, G. Galloway, V. Malik, B. Coley, K. R. Clark, J. Li, X. Xiao, J. Samulski, S. W. McPhee, R. J. Samulski, C. M. Walker, Dystrophin immunity in Duchenne's muscular dystrophy. *N. Engl. J. Med.* **363**, 1429–1437 (2010).
41. S. Eghtesad, P. A. Morel, P. R. Clemens, The companions: Regulatory T cells and gene therapy. *Immunology* **127**, 1–7 (2009).
42. M. A. Hossain, B. C. Man, C. Zhao, Q. Xu, X. J. Du, J. D. Wade, C. S. Samuel, H3 relaxin demonstrates antifibrotic properties via the RXFP1 receptor. *Biochemistry* **50**, 1368–1375 (2011).
43. A. E. Kalovidouris, Z. Plotkin, D. Graesser, Interferon-gamma inhibits proliferation, differentiation, and creatine kinase activity of cultured human muscle cells. II. A possible role in myositis. *J. Rheumatol.* **20**, 1718–1723 (1993).
44. T. O. Ishikawa, N. K. Jain, M. M. Taketo, H. R. Herschman, Imaging cyclooxygenase-2 (*Cox-2*) gene expression in living animals with a luciferase knock-in reporter gene. *Mol. Imaging Biol.* **8**, 171–187 (2006).
45. F. Boehm, M. Martin, R. Kesselring, G. Schiechl, E. K. Geissler, H. J. Schlitt, S. Fichtner-Feigl, Deletion of Foxp3$^+$ regulatory T cells in genetically targeted mice supports development of intestinal inflammation. *BMC Gastroenterol.* **12**, 97 (2012).

Acknowledgments: We thank M. Ortanez for technical assistance, D. Fuentes for animal husbandry, and T. S. for the DEREG mice. **Funding:** These studies were supported by a Ruth L. Kirschstein National Research Service Award training grant (1F32AR063575-01A1 to S.A.V.); by grants R01 AI50834, RO1 AI46643, P01 AI35297, and P30DK63720 from the U.S. NIH to J.A.B.; by the NIH in partial support for the Center for Duchenne Muscular Dystrophy, grant nos. P30AR057230-0 and U54 AR052646, by Department of Defense grant no. 6288, and by Muscular Dystrophy Association grant no. 199723 to M.J.S.; and by grants AR066817, AR047721, and AR062597 from the NIH to J.G.T. **Author contributions:** S.A.V., W.R., and L.M. performed the experiments. A.K. performed genotyping of the mice used in this study and performed flow cytometry and histological experiments. M.M. contributed to fig. S8 and table S1. T.S. provided mice and consultation regarding the DT-mediated depletion of T_{regs} in mdx^{DERG} mice. S.A.V., J.G.T., M.J.S., and J.A.B. designed all experiments. Data interpretation and assembly of the manuscript were performed by S.A.V. and J.A.B. **Competing interests:** The authors declare that they have no competing interests.

Submitted 1 July 2014
Accepted 25 September 2014
Published 15 October 2014
10.1126/scitranslmed.3009925

Citation: S. A. Villalta, W. Rosenthal, L. Martinez, A. Kaur, T. Sparwasser, J. G. Tidball, M. Margeta, M. J. Spencer, J. A. Bluestone, Regulatory T cells suppress muscle inflammation and injury in muscular dystrophy. *Sci. Transl. Med.* **6**, 258ra142 (2014).

Science Translational Medicine AAAS

Regulatory T cells suppress muscle inflammation and injury in muscular dystrophy

S. Armando Villalta *et al.*

Sci Transl Med **6**, 258ra142 (2014);
DOI: 10.1126/scitranslmed.3009925

Editor's Summary

T_{regs} Muscle In on the Action

Duchenne muscular dystrophy (DMD) is caused by mutations in the dystrophin gene leading to muscle degeneration. Villalta *et al.* now show that the imbalance between proinflammatory and proregulatory immune cells in both humans with DMD and in the mdx mouse model of the disease is directly involved in myofiber damage. Increasing the number of anti-inflammatory regulatory T cells (T_{regs}) in dystrophic muscle prevents tissue destruction and ameliorates clinical manifestations. T_{reg} elimination resulted in increased production of proinflammatory cytokines and macrophages, whereas treatment with the T_{reg}-promoting cytokine interleukin-2 (IL-2) increased immunosuppressive IL-10 production and resolved myofiber damage. Thus, this study shows that T_{regs} modulate the progression of muscular dystrophy by suppressing type 1 inflammation and highlight the potential of T_{reg}-modulating agents as DMD therapeutics.

Science Translational Medicine (print ISSN 1946-6234; online ISSN 1946-6242) is published weekly, except the last week in December, by the American Association for the Advancement of Science, 1200 New York Avenue NW, Washington, DC 20005.